Title

Patients with familial adenomatous polyposis harbor colonic biofilms containing tumorigenic bacteria.

Journal

The Scientific monthly, 359(6375)

Authors

Dejea, Christine
Fathi, Payam
Craig, John
et al.

Publication Date

2018-02-02

DOI

10.1126/science.aah3648

Peer reviewed

HHS Public Access

Author manuscript

Science. Author manuscript; available in PMC 2018 April 03.

Published in final edited form as:

Science. 2018 February 02; 359(6375): 592–597. doi:10.1126/science.aah3648.

Patients with familial adenomatous polyposis harbor colonic biofilms containing tumorigenic bacteria

Christine M. Dejea[1,2,*], **Payam Fathi**[1,2,3,†], **John M. Craig**[4], **Annemarie Boleij**[1,5], **Rahwa Taddese**[5], **Abby L. Geis**[1,2,‡], **Xinqun Wu**[1,3], **Christina E. DeStefano Shields**[1,2], **Elizabeth M. Hechenbleikner**[6,§], **David L. Huso**[7,‖], **Robert A. Anders**[8], **Francis M. Giardiello**[2,3], **Elizabeth C. Wick**[6,¶], **Hao Wang**[1,2], **Shaoguang Wu**[1,3], **Drew M. Pardoll**[1,2], **Franck Housseau**[1,2], and **Cynthia L. Sears**[1,2,3,#]

[1]Bloomberg-Kimmel Institute for Cancer Immunotherapy, Johns Hopkins University, Baltimore, MD, USA [2]Department of Oncology, Johns Hopkins University, Baltimore, MD, USA [3]Department of Medicine, Johns Hopkins University, Baltimore, MD, USA [4]Department of Environmental Health Sciences, Bloomberg School of Public Health, Johns Hopkins University, Baltimore, MD, USA [5]Department of Pathology, Radboud University Medical Center, Postbus 9101, 6500 HB Nijmegen, Netherlands [6]Department of Surgery, Johns Hopkins University, Baltimore, MD, USA [7]Department of Molecular and Comparative Pathobiology, Johns Hopkins University, Baltimore, MD, USA [8]Department of Pathology, Johns Hopkins University, Baltimore, MD, USA

Abstract

Individuals with sporadic colorectal cancer (CRC) frequently harbor abnormalities in the composition of the gut microbiome; however, the microbiota associated with precancerous lesions in hereditary CRC remains largely unknown. We studied colonic mucosa of patients with familial adenomatous polyposis (FAP), who develop benign precursor lesions (polyps) early in life. We identified patchy bacterial biofilms composed predominately of *Escherichia coli* and *Bacteroides fragilis*. Genes for colibactin (*clbB*) and *Bacteroides fragilis* toxin (*bft*), encoding secreted oncotoxins, were highly enriched in FAP patients' colonic mucosa compared to healthy individuals. Tumor-prone mice cocolonized with *E. coli* (expressing colibactin), and enterotoxigenic *B. fragilis* showed increased interleukin-17 in the colon and DNA damage in colonic epithelium with faster tumor onset and greater mortality, compared to mice with either

[#]Corresponding author. csears@jhmi.edu.
[*]Present address: 10903 New Hampshire Avenue, WO22 RM 5171, Silver Spring, MD 20993, USA.
[†]Present address: Vanderbilt University School of Medicine, 340 Light Hall, Nashville, TN 37232, USA.
[‡]Present address: Arkansas College of Osteopathic Medicine, 7000 Chad Colley Boulevard, Fort Smith, AR 72916, USA.
[§]Mount Sinai Hospital, Department of Surgery, 5 East 98th Street, New York, NY 10029, USA.
[‖]Deceased.
[¶]Present address: Department of Surgery, University of California, 513 Parnassus Avenue, S 549, San Francisco, CA 94143, USA.

SUPPLEMENTARY MATERIALS

www.sciencemag.org/content/359/6375/592/suppl/DC1

Materials and Methods
Figs. S1 to S11
Tables S1 to S7
References (15, 16)

bacterial strain alone. These data suggest an unexpected link between early neoplasia of the colon and tumorigenic bacteria.

Colorectal cancer (CRC) is very common globally and develops through accumulation of colonic epithelial cell (CEC) mutations that promote transition of normal mucosa to adenocarcinoma. Around 5% of CRC occurs in individuals with an inherited mutation (1). One hereditary condition, familial adenomatous polyposis (FAP), is caused by germline mutation in the *APC* tumor suppressor gene. Individuals with FAP are born with their first mutation in the transition to CRC, and as somatic mutations accumulate, develop hundreds to thousands of colorectal polyps. The onset and frequency of polyp formation within families bearing the same *APC* gene mutation varies substantially (2), suggesting that additional factors contribute to disease onset, including components of the microbiome (3).

The colon contains trillions of bacteria that are separated from the colonic epithelium by a dense mucus layer. This mucus layer promotes tolerance to foreign antigens by limiting bacterial–epithelial cell contact and, thus, mucosal inflammatory responses. In contrast, bacterial breaches into the colonic mucus layer with, in some, biofilm formation fosters chronic mucosal inflammation (4–6).

We previously reported that biofilms on normal mucosa of sporadic CRC patients were associated with a pro-oncogenic state (6, 7), suggesting that biofilm formation is an important epithelial event influencing CRC. To test the hypothesis that biofilm formation may be an early event in the progression of hereditary colon cancer, we examined the mucosa of FAP patients at clinically indicated colectomy.

We initially screened surgically resected tissue preserved in Carnoy's fixative from five patients with FAP and one with juvenile polyposis syndrome (table S1). Colon biopsies from individuals undergoing screening colonoscopy or surgical resections served as controls (n = 20, table S2). Polyps and macroscopically normal tissue were labeled with a panbacterial 16*S* ribosomal RNA (rRNA) fluorescence in situ hybridization (FISH) probe. Each FAP patient exhibited bacterial invasion through the mucus layer scattered along the colonic axis (Fig. 1A, table S3, and fig. S1). Unlike the continuous mucosal bio-films in sporadic CRC patients (6), FAP tissue displayed patchy bacterial mucus invasion (average length, 150 μm) on ~70% of the surgically resected colon specimens collected from four of six hereditary tumor patients. Biofilms were not restricted to polyps, nor did they display right colon geographic preference as observed in sporadic CRC (table S3 and figs. S1 and S2). Bio-films were not detected in the mucus layer of the FAP patient who received oral antibiotics 24 hours before surgery (table S1 and fig. S2).

Specimens with bacterial biofilms were further screened by additional 16*S* rRNA probes to recognize the major phyla detected in biofilms of sporadic CRC; namely, *Bacteroides/Prevotella*, *Proteobacteria*, *Lachnospiraceae*, and *Fusobacteria* (table S4). Notably, FAP biofilms were composed predominantly of mucus-invasive *Proteobacteria* (~60 to 70%) and *Bacteroides* (10 to 32%) (table S3). *Fusobacteria* were not detected, and *Lachnospiraceae* were rare (<3%) by quantitative FISH analysis (table S3).

Additional probe sets (table S4) identified the predominant biofilm members as *E. coli* and *B. fragilis* (Fig. 1A, bottom panels; table S3). Invasion of the epithelial cell layer by biofilm community members was detected in all patients harboring biofilms (Fig. 1B), a finding similar to that in sporadic CRC patients. Further, FISH of mucosal biopsies from ileal pouches or ano-rectal remnants of additional, longitudinally followed, postcolectomy FAP patients revealed biofilms in 36% and mucosal-associated *E. coli* or *B. fragilis* in 50% (table S5). Thus, *E. coli* and *B. fragilis* are frequent, persistent mucosal colonizers of the FAP gastrointestinal tract. Of note, semiquantitative colon mucosa bacterial cultures of $Apc^{Min\Delta 716/+}$ mice (truncation at the 716 codon of *Apc*), a murine correlate of FAP, displayed similar enrichment of *Bacteroides* and *Enterobacteriaceae* compared to wild-type (WT) littermates, consistent with data reported for $Apc^{Min\Delta 850/+}$ mice (fig. S3) (8). These results suggest that *Apc* mutations enhance mucosal bacterial adherence, altering the bacterial–host epithelial interaction.

Strong experimental evidence exists supporting the carcinogenic potential of molecular subtypes of both *E. coli* and *B. fragilis* (9, 10); the two dominant biofilm members identified in direct contact with host colon epithelial cells in our FAP patients. *E. coli* containing the polyketide synthase (*pks*) genotoxic island (encodes the genes responsible for synthesis of the colibactin genotoxin) induces DNA damage in vitro and in vivo along with colon tumorigenesis in azoxymethane (AOM)–treated interleukin-10 (IL-10)– deficient mice (10), whereas, enterotoxigenic *Bacteroides fragilis* (ETBF) induces colon tumorigenesis in $Apc^{Min/+}$ mice (9). Human epidemiological studies have associated ETBF and *pks*+ *E. coli* with inflammatory bowel disease and sporadic CRC (10–13). Thus, we cultured banked frozen mucosal tissues from 25 FAP patients (two polyps and two normal tissues per patient when available, table S1) and 23 healthy individuals (mucosal sample from surgical resection or one ascending and one descending colon biopsy per colonoscopy subject, table S2) for the presence of *pks*+ *E. coli* and ETBF. The mucosa of FAP patients was significantly associated with *pks*+ *E. coli* (68%) and ETBF (60%) compared to healthy subject mucosa (22% *pks*+ *E. coli* and 30% ETBF) (Fig. 1C). There was no preferential association of ETBF or *pks*+ *E. coli* with polyp or normal mucosa from FAP patients. Typically, mucosal samples from individual patients were concordant for *pks*+ *E. coli* or ETBF (73% for *pks*+ *E. coli*, 59% for ETBF), similar to results for mucosal *bft* detection in sporadic CRC patients (13). Notably, *pks*+ *E. coli* and ETBF mucosal coassociation occurred at a higher rate (52%) than expected to occur randomly (40.8%) given the frequencies for the individual species (Fig. 1C). Increased mucosal coassociation also occurred in healthy control subjects (22% observed versus 6.6% expected) (Fig. 1C). Laser capture micro-dissection of mucosal biofilms from our initial FAP patients (fig. S2 and table S1) contained both *bft* and *clbB* as determined by polymerase chain reaction (PCR) analysis, indicating that the carcinogenic subtypes of *B. fragilis* and *E. coli*, respectively, were present in the mucus layer in direct contact with the FAP epithelium (Fig. 1D). In contrast, neither virulence gene was detected in the mucus layer of control subject 3760 whereas *bft* was detected in the mucus layer of control subject 3730, consistent with our prior reported culture analysis of this sample (Fig. 1D) (13).

The high frequency of *pks*+ *E. coli* and ETBF cocolonization in FAP colons highlights the importance of understanding the potential effects of simultaneously harboring these two

carcinogenic bacteria. Consequently, we used two murine models, AOM treatment without dextran sodium sulfate (see materials and methods) and $Apc^{Min\Delta 716/+}$ mice to test the hypothesis that *pks*+ *E. coli* and ETBF cocolonization enhances colon tumorigenesis compared to monocolonization with either bacterium. The rate of spontaneous colon tumorigenesis is very low in both model systems.

Specific pathogen-free wild-type mice were treated with the carcinogen AOM and monoinoculated or coinoculated with canonical strains of *pks*+ *E. coli* (the murine adherent and invasive strain, NC101) and ETBF (strain 086-5443-2-2) (9, 10). Fecal ETBF or *pks*+ *E. coli* colonization was similar under monocolonization or cocolonization conditions, persisting until colon tumor formation was assessed at 15 weeks after colonization (fig. S4). Monocolonized (*pks*+ *E. coli* or ETBF) mice displayed few to no tumors. However, pronounced tumor induction occurred in cocolonized mice, including an invasive cancer, suggesting the requirement for both bacteria to yield oncogenesis (Fig. 2, A to C). Tumorigenesis required the presence of BFT and the colibactin genotoxin as in-frame deletions of the *bft* gene and the *pks* virulence island significantly decreased tumors (Fig. 2A).

$Apc^{Min\Delta 716/+}$mice cocolonized with ETBF and *pks*+ *E. coli* exhibited enhanced morbidity with rapid weight loss and significantly increased mortality ($P < 0.0001$) [loss of 80% of the mice ($n = 8$) by 8 weeks and the remaining 20% ($n = 2$) at 12 weeks after colonization]. In contrast, 90% ($n = 9$) and 100% ($n = 10$) of mice monocolonized with ETBF or *pks*+ *E. coli*, respectively, survived 15 weeks after colonization (Fig. 2D). The robust tumorigenesis of ETBF alone (at 15 weeks) and cocolonized mice (majority deceased by 8 weeks after colonization) was similar, whereas tumor numbers were significantly increased in the cocolonized cohort compared to *pks*+ *E. coli* alone (fig. S5). Notably, at early time points, inflammation was increased in the cocolonized cohort compared to either ETBF or *pks*+ *E. coli* alone (fig. S5). Together these results suggest that the significant increase in colon inflammation and early tumorigenesis in the cocolonized mice contributed to their earlier mortality in the $Apc^{Min/+}$ mouse model.

Consistent with enhanced tumorigenesis, histopathological analysis revealed significantly increased colon hyperplasia and mucosal micro-adenomas in cocolonized AOM-treated mice compared to monocolonized mice (Fig. 3A and fig. S6A). However, histopathology scoring revealed modest differences in inflammation over time (4 days to 15 weeks) in mono- and cocolonized AOM mice (Fig. 3B and fig. S6B). Thus, overall inflammation did not seem to explain differential tumor induction. To determine if the type of inflammation contributed to differences in tumorigenesis, we analyzed lamina propria immune-cell infiltrates of monocolonized and cocolonized wild-type AOM mice by flow cytometry. Our general lymphoid panel revealed a marked B cell influx across all colonization groups (Fig. 3C) but no significant differences in the proportion of infiltrating T cells (CD4, CD8, or γδ T cells) and myeloid populations between monocolonized and cocolonized AOM mice (Fig. 3C) either at the acute (1-week) or chronic (3-week) stage of infection.

Of particular interest was IL-17, as the tumorigenic potential of ETBF in $Apc^{Min\Delta 716/+}$ mice has been attributed, in part, to IL-17 (9). Because *bft* was necessary for synergistic tumor

induction under cocolonization conditions (Fig. 2A), we tested the role of IL-17 in the cocolonized AOM model. Although IL-17 expression analysis by quantitative PCR revealed no significant difference in overall mucosal IL-17 mRNA levels between 15-week ETBF monocolonized and ETBF and *pks+ E. coli* cocolonized mice (fig. S7), cocolonization of IL-17–deficient AOM mice ablated tumorigenesis (Fig. 3D). To specifically test whether ETBF and *pks+ E. coli* cocolonization affected early colon mucosal IL-17 production, germ-free C57BL/6 mice were mono- or cocolonized and innate and adaptive lymphocyte subsets analyzed by flow cytometry. Germ-free mice cocolonized with ETBF and *pks+ E. coli* displayed a trend toward increase in total mucosal IL-17–producing cells when compared to monocolonized ETBF or *pks+ E. coli* mice, driven by both adaptive [T helper 17 (T_H17)] and innate (particularly γδT17) cells (Fig. 3E and table S7). Although necessary for tumorigenesis (Fig. 3D), IL-17 alone appears insufficient to explain synergistic tumorigenesis in cocolonized mice because robust IL-17 induction by ETBF monocolonization (fig. S7) induces only meager colon tumorigenesis in AOM mice (Fig. 2A).

Because our general lymphoid panel revealed a marked B cell influx across all colonization groups (Fig. 3C), we profiled the secretory immunoglobulin A (IgA) response by IgA enzyme-linked immunosorbent assay (ELISA) using stool collected 4 weeks after colonization from AOM mice. Cocolonized mice had a significantly more robust IgA response to *pks+ E. coli* than mice monocolonized with *pks+ E. coli*, whereas the fecal anti-ETBF IgA response was similar under mono- and cocolonization conditions (Fig. 4A). Thus, the increased fecal IgA response was specific to *pks+ E. coli* in mice cocolonized with ETBF, suggesting that cocolonization enhanced mucosal exposure to *pks+ E. coli*.

Although fecal colonization of both *pks+ E. coli* and ETBF was equivalent under both mono- and cocolonization conditions (fig. S4), quantification of mucosal-adherent ETBF and *pks+ E. coli* revealed a marked increase in mucosal-adherent *pks+ E. coli* under cocolonization conditions compared to *pks+ E. coli* monocolonization (Fig. 4B). Hence, under monocolonization conditions, *pks+ E. coli* is largely cultivatable only from the colon lumen whereas in the presence of ETBF, *pks+ E. coli* colonizes the mucosa at high levels (10^3 to 10^6 colony-forming units per gram of tissue). Using Muc-2–producing HT29-MTX-E12 monolayers in vitro, we tested the impact of *pks+ E. coli* and ETBF on mucus. Although *pks+ E. coli* colonization alone had no impact on mucus depth, monolayer colonization with ETBF alone or cocolonized with *pks+ E. coli* significantly reduced mucus depth similar to colonization with *A. muciniphila* a known human colonic mucin-degrading bacterium (Fig. 4C). These results suggest that mucus degradation by ETBF promotes enhanced *pks+ E. coli* colonization. Such a shift in the bacterial niche of *pks+ E. coli* would facilitate the delivery of colibactin, the DNA-damaging toxin released by *pks+ E. coli*, to colon epithelial cells. Consistent with this hypothesis, γ-H2AX immunohistochemistry revealed significantly enhanced DNA damage in the colon epithelial cells of AOM mice cocolonized with *pks+ E. coli* and ETBF compared to monocolonized (*pks+ E. coli* or ETBF) mice (Fig. 4D). Further, mice cocolonized with ETBF and *E. coliΔpks* displayed similarly enhanced mucosal colonization with the *E. coli* strain (fig. S8) but reduced tumors and no increase in DNA damage or IL-17 (Fig. 2A and fig. S9, A and B, respectively). Lastly, persistent cocolonization of AOM-treated mice with the mucin-degrading *A.*

muciniphila and *pks+ E. coli* did not enhance, but rather reduced, the modest colon tumorigenesis (fig. S10, A and B) induced by *pks+ E. coli* monocolonization. These results suggest that mucus degradation alone was insufficient to promote *pks+ E. coli* colon carcinogenesis in AOM mice.

Taken together, these data suggest that co-colonization with ETBF and *pks+ E. coli*, found in more than half of FAP patients (in contrast to less than 25% of controls), promotes enhanced carcinogenesis through two distinct but complementary steps: (i) mucus degradation enabling increased *pks+ E. coli* adherence, inducing increased colonic epithelial cell DNA damage by colibactin (Fig. 4D and fig S9); and (ii) IL-17 induction promoted, primarily, by ETBF with early augmentation by *pks+ E. coli* cocolonization (Fig. 3, D and E, and table S7). We propose that together these mechanisms yield cooperative tumor induction in AOM mice cocolonized with ETBF and *pks+ E. coli*.

ETBF and *pks+ E. coli* commonly colonize young children worldwide. Thus, our results suggest that persistent cocolonization in the colon mucosa from a young age may contribute to the pathogenesis of FAP and potentially even those who develop sporadic CRC because *APC* loss or mutation occurs in the vast majority of sporadic CRC. We note that *pks+ E. coli* are phenotypic and genotypic adherent and invasive *E. coli* (AIEC) (14). Despite this designation, derived primarily from in vitro cell culture experiments, the canonical *pks+ E. coli* strain (NC101) used in our experiments was only cultivatable from the colon lumen in the absence of concomitant ETBF colonization in our mouse model. This ETBF-dependent shift to marked mucosal *pks+ E. coli* colonization is consistent with our observations that ETBF and *pks+ E. coli* cocolonize FAP colon biofilms, where both bacteria invade and cocolonize the mucus layer throughout the FAP colon. These findings suggest that analysis of coexpression of *bft* and *clbB* may have value in general screening and potential prevention of CRC.

Supplementary Material

Refer to Web version on PubMed Central for supplementary material.

Acknowledgments

We thank K. Kinzler and B. Vogelstein for valuable discussions; K. Romans and L. Hylind for assistance with patient enrollment; and S. Besharati for assistance with histopathologic analyses. The data presented in this manuscript are tabulated in the main text and supplementary materials and methods. This work was supported by the Bloomberg Philanthropies and by NIH grants R01 CA151393 (to C.L.S., D.M.P.), K08 DK087856 (to E.C.W.), 5T32CA126607-05 (to E.M.H.), P30 DK089502 (Johns Hopkins University School of Medicine), P30 CA006973 (Johns Hopkins University School of Medicine), and P50 CA62924 (Johns Hopkins University School of Medicine). Funding was also provided through a research agreement with Bristol-Myers Squibb Co-International Immuno-Oncology Network-IION Resource Model, 300-2344 (to D.M.P.); Alexander and Margaret Stewart Trust (Johns Hopkins University School of Medicine); GSRRIG-015 (American Society of Colon and Rectal Surgeons to E.M.H.); The Netherlands Organization for Scientific Research (NWO 825.11.03 and 016.166.089 to A.B.); and a grant from the Institute Mérieux (to C.L.S. and D.M.P.). D.M.P. discloses consultant relationships with Aduro Biotech, Amgen, Astra Zeneca, Bayer, Compugen, DNAtrix, Five Prime, GlaxoSmithKline, ImmuneXcite, Jounce Therapeutics, Neximmune, Pfizer, Rock Springs Capital, Sanofi, Tizona, Janssen, Merck, Astellas, Flx Bio, Ervaxx, and DNAX. D.M.P. receives research support from Bristol-Myers Squibb, Compugen, Ervaxx, and Potenza. D.M.P. is a scientific advisory board member for Immunomic Therapeutics. D.M.P. shares intellectual property with Aduro Biotech, Bristol-Myers Squibb, Compugen, and Immunomic Therapeutics. All other authors declare no competing interests. C.L.S., D.M.P., C.M.D., and E.C.W. are inventors on patent application PCT/US2014/055123 submitted by Johns Hopkins University that covers use of biofilm formation to define risk for colon cancer.

REFERENCES AND NOTES

1. Fearon ER, Vogelstein B. Cell. 1990; 61:759–767. [PubMed: 2188735]
2. Giardiello FM, et al. Gastroenterology. 1994; 106:1542–1547. [PubMed: 8194700]
3. Dejea C, Wick E, Sears CL. Future Microbiol. 2013; 8:445–460. [PubMed: 23534358]
4. Swidsinski A, et al. Gut. 2007; 56:343–350. [PubMed: 16908512]
5. Swidsinski A, Loening-Baucke V, Herber A. J Physiol Pharmacol. 2009; 60(suppl 6):61–71.
6. Dejea CM, et al. Proc Natl Acad Sci USA. 2014; 111:18321–18326. [PubMed: 25489084]
7. Johnson CH, et al. Cell Metab. 2015; 21:891–897. [PubMed: 25959674]
8. Son JS, et al. PLOS ONE. 2015; 10:e0127985. [PubMed: 26121046]
9. Wu S, et al. Nat Med. 2009; 15:1016–1022. [PubMed: 19701202]
10. Arthur JC, et al. Science. 2012; 338:120–123. [PubMed: 22903521]
11. Prindiville TP, et al. Emerg Infect Dis. 2000; 6:171–174. [PubMed: 10756151]
12. Prorok-Hamon M, et al. Gut. 2014; 63:761–770. [PubMed: 23846483]
13. Boleij A, et al. Clin Infect Dis. 2015; 60:208–215. [PubMed: 25305284]
14. Martinez-Medina M, et al. J Clin Microbiol. 2009; 47:3968–3979. [PubMed: 19828750]

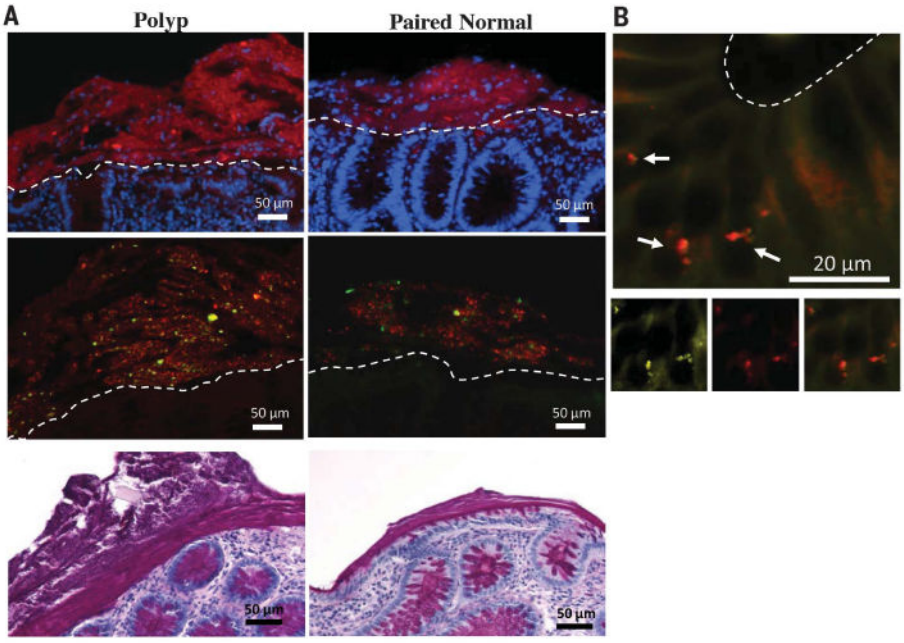

C

Presence of *pks+ E. coli* and ETBF on colon mucosa of FAP patients and Controls					
Total		***pks+ E. coli***	**ETBF**	***pks+E. coli*,** **ETBF**	**Neither**
FAP	25	17 (68%)	15 (60%)	13 (52%)	6 (24%)
Controls	23	5 (22%)	7 (30%)	5 (22%)	16 (70%)
p value		0.002	0.049	0.0400	0.0030

Fig. 1. Fluorescent in situ hybridization (FISH) and microbiology culture analysis of FAP mucosal tissues

(**A**) Top panels: Representative FISH images of bacterial biofilms (red) on the mucosal surface of a FAP polyp and paired normal tissues counterstained with DAPI (4′,6-diamidino-2-phenylindole) nuclear stain (blue). Middle panels: Most of the biofilm composition was identified as *B. fragilis* (green) and *E. coli* (red) by using species-specific probes. Bottom panels: PAS (periodic acid–Schiff)–stained histopathology images of polyp and paired normal mucosal tissues demonstrating the presence of the mucus layer. Images were obtained at 40× magnification; scale bars, 50 μm. Dotted lines delineate the luminal edge of the colonic epithelial cells. Images are representative of $n = 4$ to 23 tissue samples per patient screened (at least 10 5-μm sections screened per patient). (**B**) *Enterobacteriaceae* (yellow) and *E. coli* (red) FISH probes on paired normal FAP tissue (100× magnification) revealing invasion into the epithelial cell layer at the base of a crypt (arrows). Bottom panels with insets of *Enterobacteriaceae* (bottom left panel) in yellow, *E. coli* (bottom middle panel) in red, and overlay (bottom right panel) confirming identification of the invasive species. Scale bar, 20 μm. Images are representative of $n = 5$ to 16 tissue samples per patient screened (at least 10 5-μm sections screened per patient). (**C**) FAP and control prevalence of *pks+ E. coli* and enterotoxigenic *Bacteroides fragilis* (ETBF). Chi-square *P*-values are shown that represent the difference in probability of detection of each bacterium in FAP versus control patients. (**D**) PCR detection of *clbB* (a gene in the *pks* island) and *bft* within laser-captured biofilms containing *E. coli* and *B. fragilis* from designated FAP patients (table

S1) and controls (table S2; materials and methods). Data show a representative image from two independent experiments with two or three replicates per experiment performed.

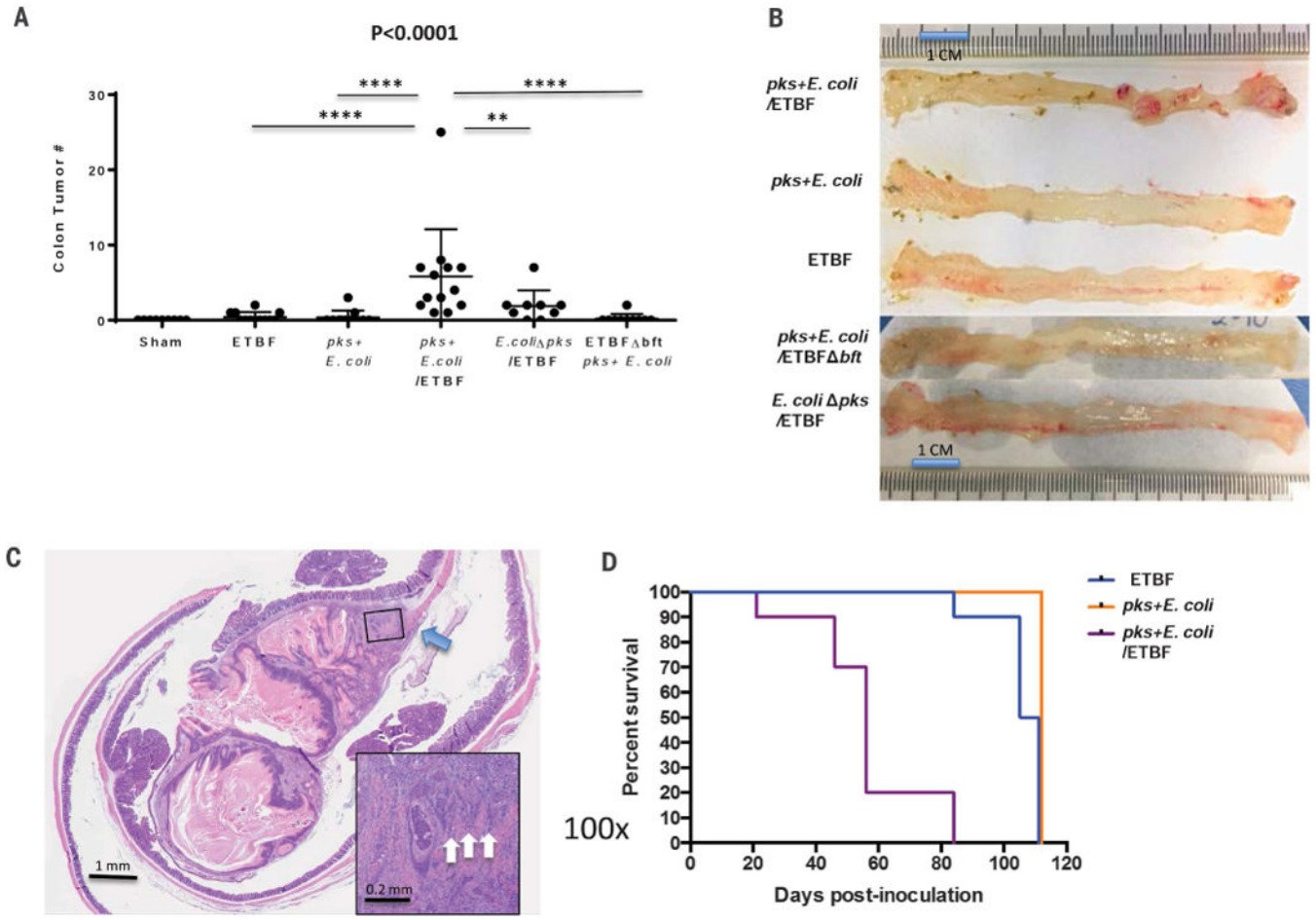

Fig. 2. Cocolonization by *pks+ E. coli* and ETBF increases colon tumor onset and mortality in murine models of CRC

(**A**) Total colon tumor numbers detected in sham ($n = 9$), ETBF monocolonized ($n = 12$), *pks+E. coli* monocolonized ($n = 11$), *pks+ E. coli*/ETBF cocolonized ($n = 13$), *E. coli*Δ*pks*/ETBF ($n = 9$), or *pks+ E. coli*/ETBFΔ*bft* ($n = 10$) AOM mice at 15 weeks after colonization. Data indicate mean ± SEM. Overall significance was calculated with the Kruskal-Wallis test, and the overall P value is shown; Mann-Whitney U was used for two-group comparisons; $^{**}P = 0.016$, $^{****}P < 0.0001$. (**B**) Representative colons of monocolonized (ETBF or *pks+ E. coli*), cocolonized (ETBF/*pks+ E. coli*), *E. coli*Δ*pks*/ETBF, and *pks+ E. coli*/ETBFΔ*bft* mice at 15 weeks after colonization of AOM-treated mice. Images are representative of $n = 9$ to 13 mice for each group. (**C**) H&E (hematoxylin and eosin) histopathology of an invasive adenocarcinoma in a cocolonized (*pks+ E. coli*/ETBF) AOM mouse at 15 weeks. Main image, 10× magnification; scale bar, 1 mm. Inset image, 100× magnification; scale bar, 0.2 mm. Blue arrow depicts the disruption of the muscularis propria by the invasive adenocarcinoma, and white arrows (inset) identify invading clusters of adenocarcinoma epithelial cells. (**D**) Kaplan-Meir survival plot of $Apc^{\Delta 716Min/+}$ mice ($n = 30$) colonized with either ETBF (blue; $n = 10$), *pks+ E. coli* (orange; $n = 10$), or cocolonized with *pks+ E. coli* and ETBF (purple; $n = 10$). Cocolonization significantly ($P < 0.0001$) increased the

mortality rate. Statistics were analyzed with the log-rank test. All surviving mice ($n = 19$) were harvested at 110 days.

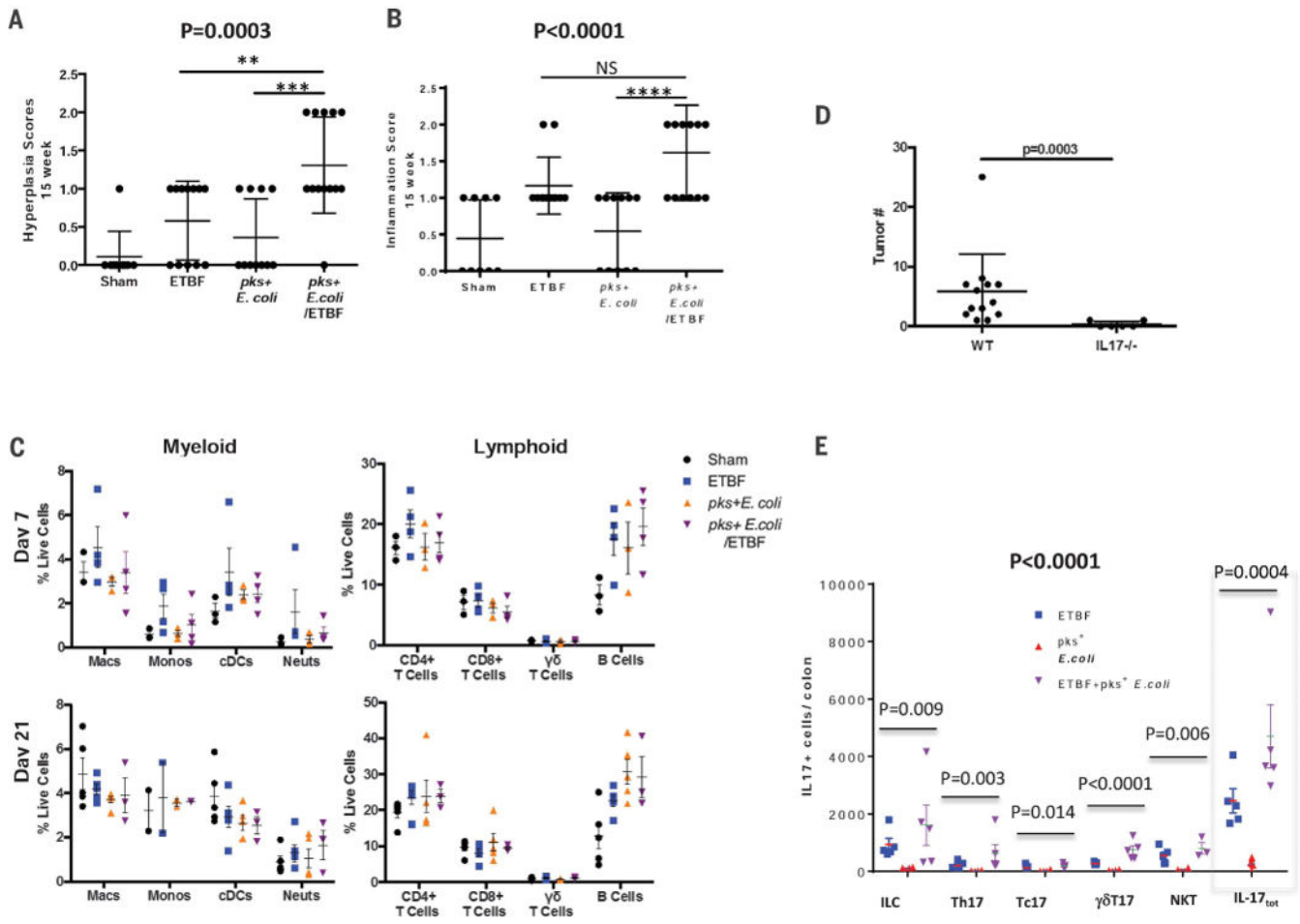

Fig. 3. IL-17–induced inflammation is necessary for bacterial-driven tumorigenesis

(**A**) Histologic hyperplasia and (**B**) inflammation scores of 15-week AOM sham ($n = 9$), ETBF monocolonized ($n = 12$), *pks+ E. coli* monocolonized ($n = 11$), or *pks+ E. coli*/ETBF cocolonized ($n = 13$) mice. Data represent mean ± SEM of three independent experiments. For (A) and (B), overall significance was calculated by using the Kruskal-Wallis test, and the overall P value is shown; Mann-Whitney U was used for two-group comparisons; $^{**}P = 0.01$, $^{***}P = 0.0014$, $^{****}P = 0.0006$; NS, not significant. (**C**) Myeloid and lymphoid lamina propria immune cell infiltrates plotted as percentage of live cells in AOM mice at day 7 (top panels) and day 21 (bottom panels) after colonization. Data represent mean ± SEM of three independent experiments (total three to five mice per group). (**D**) Total tumor numbers detected in IL-17–deficient AOM-treated mice ($IL17^{-/-}$) versus wild-type AOM mice (WT). Both mouse strains were cocolonized with *pks+ E. coli* and ETBF and tumors assessed at 15 weeks. Data represent mean ± SEM of two or three independent experiments (total 6 to 13 mice per group). Significance calculated by the Mann-Whitney U test represents differences between the non-normally distributed colon tumors in the independent mouse groups. (**E**) IL-17–producing cell subsets and total number of IL-17–producing (IL-17tot) cells per colon harvested from germ-free C57BL/6 mice monocolonized with *pks+ E. coli* or ETBF or cocolonized with *pks+ E. coli* and ETBF for up to 60 hours. Data represent mean ± SEM of two independent experiments (total 3 to 5 mice per group). Overall significance across

IL-17–producing cell types was calculated by using two-way analysis of variance testing based on log-transformed data (bold *P* value). For each cell subset and total number of IL-17–producing cells (gray dotted line box), the overall *P* value is shown and was calculated by using the Kruskal-Wallis test. Two-group cell subset and total number of IL-17–producing cell comparisons were analyzed by Mann-Whitney U test and are reported in table S7.

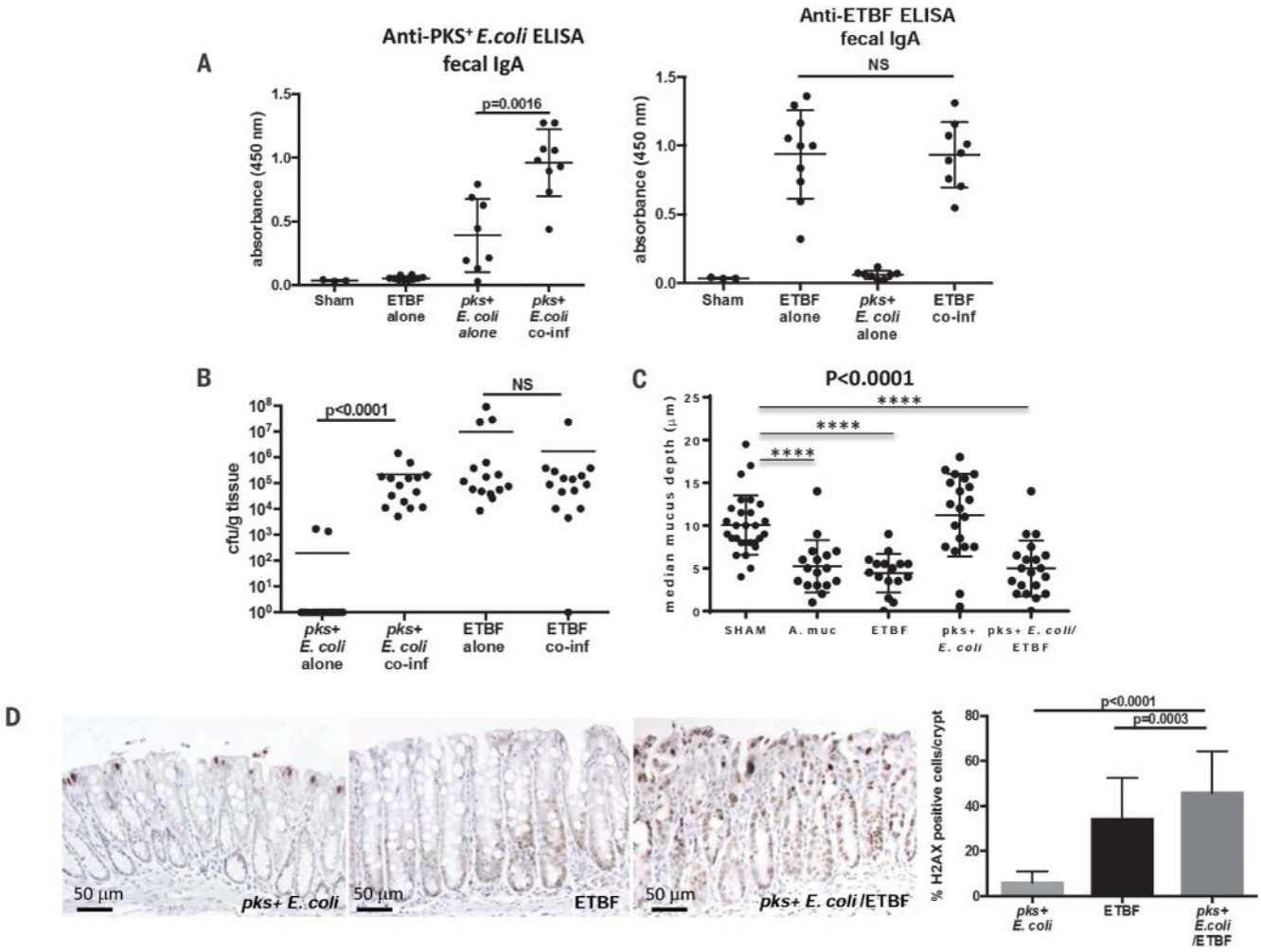

Fig. 4. ETBF enhances *pks+ E. coli* colonization and colonic epithelial cell DNA damage

(**A**) ELISA results showing anti-*pks+ E. coli* (NC101) IgA and anti-ETBF (86-5443-2-2) IgA present in fecal supernatants from wild-type AOM mice under the designated colonization conditions for 4 weeks. Data represent mean ± SEM of three independent experiments (total 3 to 10 mice per group). (**B**) Colonization of distal colon mucosae by *pks + E. coli* and ETBF under mono- and cocolonization conditions at 4 weeks in AOM mice. Data represent mean of three independent experiments (total of 15 mice per group). (**C**) Mucus depth (μm) of HT29-MTX-E12 monolayers under the designated colonization conditions. Data represent mean ± SEM of three independent experiments. A. muc, *Akkermansia muciniphila*. (**D**) Representative images of γ-H2AX immunohistochemistry of distal colon crypts from AOM mice (five mice per condition) mono- or cocolonized with *pks + E. coli* and ETBF for 4 days with quantification (right panel) of γ-H2AX–positive cells displayed as percentage positive per crypt (see materials and methods). Data represent mean ± SEM of three independent experiments. For (A), (B), and (D), significance was calculated with the Mann-Whitney U test for two-group comparisons; for (C), overall significance was calculated with the Kruskal-Wallis test and the overall *P* value is shown; Mann-Whitney U was used for two-group comparisons; ****$P < 0.0001$.